Unstable Periodic Orbits and Transport Properties of Nonequilibrium Steady States

William N. Vance
Institute of Theoretical Dynamics, University of California, Davis, California 95616
(Received 13 June 1991)

Nonequilibrium steady-state flows governed by time-reversible equations of motion are described in terms of unstable periodic orbits. Important properties, such as transport coefficients and the multifractal spectrum, are related to the difference in probability of observing periodic orbits and their time reverses. We apply the theory of the periodic Lorentz gas driven by a constant external field and numerically calculate the conductivity.

PACS numbers: 05.60.+w, 05.45.+b, 05.70.Ln

Several recent studies have been devoted to the relationship between transport properties and dynamical instability in deterministic systems [1-3]. In order to study deterministic nonequilibrium flows various modifications of Hamiltonian mechanics have been devised which preserve time reversibility [4-7]. Numerical simulation of nonequilibrium steady states with such equations of motion show in every case that the solution settles onto a strange attractor of lower (Liapunov) dimension than that of the phase space [8-10]. That is, the sum of the Liapunov exponents for nonequilibrium attractors is always negative, corresponding to the contraction of phase-space volume elements. It has been shown that the sum of Liapunov exponents for nonequilibrium steady states is also related to macroscopic transport coefficients [6-10]. The simplest known nonequilibrium steady-state problem with reversible equations of motion is a variant of the Lorentz gas in which a point particle moves, with constant kinetic energy, through a regular lattice of scatterers under the influence of an external field. For a fixed value of an applied field, the instantaneous current is proportional to the divergence of the vector field. Thus the average current is proportional to the sum of the Liapunov exponents. The basis of our approach relies on recent results showing how sets of longer and longer periodic orbits that are embedded in the attractor form a natural hierarchy of increasingly better approximants to the invariant set [11-15]. Since the equations of motion are time reversible, each periodic orbit has a time-reversed orbit realized in the system along which transport is in the opposite direction. In this Letter we show how macroscopic flow, transport coefficients, Einstein relations, and multifractal properties of nonequilibrium steady states can be described in terms of the difference in probability of observing periodic orbits and their time reverses.

We shall illustrate the main ideas with the isokinetic hard-disk Lorentz gas, which has become a standard model in the field [16,17]. In this model a point particle moves through an infinite triangular lattice of hard disks of diameter σ under the influence of a constant external field E in the x direction and a time-varying constraint force F_c. The constraining force maintains the system at a constant kinetic energy and makes a steady state possible. This problem is three dimensional, with two coordinates $\{x,y\}$ specifying the position of the particle and a third coordinate θ giving the angle between the velocity vector and the x axis, $\mathbf{p}=(p\cos\theta, p\sin\theta)$ (see Fig. 1). In between collisions the equations of motion are

$$\dot{x}=(p/m)\cos\theta,\quad \dot{y}=(p/m)\sin\theta,\quad \dot{\theta}=-(E/p)\sin\theta\,, \qquad (1)$$

which can be integrated analytically. The point particle undergoes elastic collisions with the disks. Using the kinetic-theory definition of temperature, we define $p^2/m=k_BT\equiv\beta^{-1}$. The equations of motion possess time-reversal symmetry; i.e., the velocity field changes into the opposite field under the involution $\mathcal{T}$: $(x,y,\theta)\to(x,y,\theta-\pi)$. Let ϕ_t denote the flow in phase space given by the solution to the equations of motion: $\phi_t(x(s),y(s),\theta(s))=(x(s+t),y(s+t),\theta(s+t))$. Symmetry under time reversal means [18]

$$\phi_{-s}=\mathcal{T}\circ\phi_s\circ\mathcal{T}\,.$$

The triangular lattice can be tiled with hexagonal cells; see Fig. 1. Motion of the particle can be restricted to the reduced configuration space of a single cell by identifying opposite sides of the hexagon. When the particle reaches a boundary of the hexagon, we transfer it to the opposite side through parallel translation of the side before continuing the trajectory. A natural Poincaré section Σ of the billiard flow is the two-dimensional collision surface $x^2+y^2=\sigma^2/4$. Coordinates on the collision surface can be chosen to be two angles defining the collision $\{\psi,\theta\}$, where ψ and θ describe the position and velocity immedi-

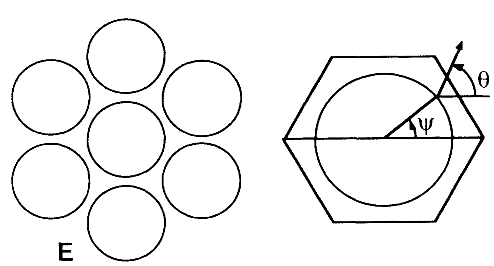

FIG. 1. The geometry of the scatterers in the Lorentz gas. A collision is specified by the two angles ψ and θ.

ately following a collision. The Poincaré mapping F takes an initial state (ψ_i,θ_i) to the state immediately following the next collision $(\psi_{i+1},\theta_{i+1})$, where i is an integer index indicating the collision number.

With the external field E applied, an average current $\langle \mathbf{v}\rangle = \langle \mathbf{p}/m\rangle$ in the positive x direction $\langle v_x\rangle$ is observed. The transport coefficient in our example is conductivity κ, which is defined at a steady state through the relation $\langle v_x\rangle = \kappa(E)E$. From the average of the divergence of the vector field we obtain a relation between $\langle v_x\rangle$ and the sum of the Liapunov exponents: $\langle v_x\rangle = -(\lambda_1+\lambda_2)/\beta E$ (we have omitted the trivial zero Liapunov exponent from the sum). Restricting this expression to a periodic orbit i, one obtains that the time average of v_x over the orbit is proportional to the sum of the Liapunov exponents of the orbit:

$$\langle v_x\rangle_i = \Delta x_i/\tau_i = -(\lambda_{1i}+\lambda_{2i})/\beta E\,, \qquad (2)$$

where $\Delta x_i = x(\tau_i) - x(0)$ is the distance along the x axis of the orbit in the (x,y) plane, and τ_i is the period of the orbit.

It is well known [11–15] that a chaotic set $\mathcal{A}$ can be hierarchically approached through sets of progressively longer unstable periodic orbits (UPOs). All prime UPOs (orbits that do not retrace themselves) of n collisions form a set $\mathcal{P}_n$, whose size increases exponentially with n. As n is increased $\mathcal{P}_n$ more closely approximates $\mathcal{A}$ in that smaller and smaller regions of phase space will be visited by orbits of $\mathcal{P}_n$. As a result of the periodicity of cells in configuration space a periodic orbit of (1) must satisfy

$$\Delta x = M\sqrt{3}R/2,\quad \Delta y = NR/2\,, \qquad (3)$$

where M and N are integers, and R is the distance between disk centers. The number of disks an orbit climbs in the x and y directions is characterized by the winding vector (M,N). To each orbit with nonzero winding vector $(M,N)\neq(0,0)$ corresponds a reverse orbit under time reversal with winding vector $(-M,-N)$. We divide $\mathcal{P}_n$ into three sets: the set of all UPOs that do not transport mass in the x direction, $M=0$, denoted by $\mathcal{P}_{n0}$, and the set of all forward (reverse) UPOs that transport mass in the positive (negative) x direction, $M>0$ $(M<0)$, denoted by $\mathcal{P}_{n+}$ $(\mathcal{P}_{n-})$. Because of the reversibility of the equations of motion, $\mathcal{P}_{n-}$ can be obtained from $\mathcal{P}_{n+}$ through the reversing involution $\mathcal{T}$; the Liapunov exponents of a reversed orbit are minus those of the forward orbit. Note from (2) that for $E\neq 0$, the Liapunov spectra of orbits in $\mathcal{P}_{n+}$ and $\mathcal{P}_{n-}$ are not symmetric about the origin.

Consider the ith periodic orbit in the set $\mathcal{P}_n$. The Liapunov numbers $\Lambda_{1i}(E)$ and $\Lambda_{2i}(E)$ of the orbit are defined as the magnitudes of the eigenvalues of the linearized nth iterate of the collision map: $\Lambda_{1i}(E) = \exp[\lambda_{1i}(E)\tau_i(E)] > 1$ and $\Lambda_{2i}(E) = \exp[\lambda_{2i}(E)\tau_i(E)] < 1$, where we have ordered the Liapunov exponents $\lambda_1 > 0 > \lambda_2$. The probability of observing a particular periodic orbit in a steady state is inversely proportional to the expanding Liapunov number Λ_1 of the orbit. The nth-order approximant to the average value of a function $g(x,y,\theta)$ thus can be written as [11]

$$\langle g\rangle_{(n)} = \sum_{i\in\mathcal{P}_n} \mathcal{G}_i(E)\Lambda_{1i}^{-1}(E) \Big/ \sum_{i\in\mathcal{P}_n} \tau_i(E)\Lambda_{1i}^{-1}(E)\,, \qquad (4)$$

where $\mathcal{G}_i(E)$ is the integral of g over orbit i, $\int_0^{\tau_i(E)} g(\phi_s X)ds$ with X on i. The function g may be separated into an even $g^{(e)}$ and an odd function $g^{(o)}$ under time reversal, $g^{(e)} = [g(x,y,\theta) + g(x,y,\theta-\pi)]/2$ and $g^{(o)} = [g(x,y,\theta) - g(x,y,\theta-\pi)]/2$. For an odd function $g^{(o)}$, nonzero contributions to the numerator come from x-climbing UPOs $\mathcal{P}_{n+}$ and $\mathcal{P}_{n-}$. In this case the numerator can be simplified by grouping each orbit with its reversed image and using (2) we obtain

$$\langle g^{(o)}\rangle_{(n)} = \sum_{i\in\mathcal{P}_{n+}} \mathcal{G}_i^{(o)}\Lambda_{1i}^{-1}(E)\{1-\exp[-\beta E\Delta x_i(E)]\} \Big/ \sum_{i\in\mathcal{P}_n} \tau_i(E)\Lambda_{1i}^{-1}(E)\,. \qquad (5)$$

Hence for $E>0$, each forward UPO that contributes is weighted more heavily than its time reverse in the sum (5). This microscopic bias of forward over reverse UPOs results in a nonzero contribution to the average value of $g^{(o)}$.

Approximants to the current, $\langle v_x\rangle$, are obtained from (5) with $\mathcal{G}_i = \mathcal{G}_i^{(o)} = \Delta x_i$. In the limit $E\to 0$, forward and reverse orbits contribute positive and negative infinities to the conductivity $\kappa(0) = \lim_{E\to 0}\langle v_x\rangle/E$. However, as seen from (5) expanded to first order in E, these infinities cancel and a positive finite value for the limiting conductivity is obtained. Writing the numerator in this expansion for $\kappa(0)$ as a sum over UPOs in $\mathcal{P}_n$, we obtain

$$\frac{\kappa(0)}{\beta} = \lim_{n\to\infty}\frac{1}{2}\frac{\sum_{i\in\mathcal{P}_n}\Delta x_i^2(0)\Lambda_{1i}^{-1}(0)}{\sum_{i\in\mathcal{P}_n}\tau_i(0)\Lambda_{1i}^{-1}(0)}\,. \qquad (6)$$

One realizes that the right-hand side of (6) is just the periodic orbit expansion of the relation for the diffusion coefficient $\mathcal{D} = \lim_{t\to\infty}\langle[x(t)-x(0)]^2\rangle/2t$. Thus the familiar Einstein relation between the diffusion coefficient and the conductivity, $\mathcal{D} = \kappa(0)/\beta$, is obtained directly from the nonequilibrium invariant measure.

To illustrate our arguments, we consider the above Lorentz gas problem with a density of $\frac{4}{5}$ the close-packed density, for which the free path of the particle is bounded, and a field strength $E = 0.01p^2/m\sigma$. We stress that UPOs can be used to characterize systems arbitrarily far from equilibrium. A small value of E was chosen to demonstrate the usefulness of the UPO approximation method in a regime where direct calculation of κ through time averaging is unfeasible due to the enormous number

TABLE I. Convergence of the prime UPO expansion for the current as a function of the UPO collision length n. M_n denotes the number of prime UPOs with n collisions.

n	M_n	$\sum\Lambda^{-1}$	$10^3\sum\Delta x\Lambda^{-1}$	$\sum\tau\Lambda^{-1}$	$\kappa_{(n)}p/m\sigma$
2	24	1.4525	1.1388	0.6042	0.1885
3	56	0.2265	0.0469	0.1089	0.0431
4	114	0.3468	0.3747	0.2580	0.1452
5	236	0.1698	0.0850	0.1347	0.0631
6	604	0.1969	0.2487	0.1955	0.1272
7	1650	0.1183	0.1124	0.1258	0.0893

of collisions needed to obtain an accurate value. We find all UPOs with n collisions with the following procedure. First, approximate UPOs are located by scanning a large time series of collisions for pairs of points separated by n collisions that are within a small preassigned distance of one another [19]. Then starting at each approximate UPO [n points on the collision surface, (ψ_i,θ_i), $i=1,\ldots,n$], we solve for a UPO using the Newton-Raphson iteration scheme applied to the $2n$-dimensional system of equations $F(\psi_i,\theta_i)-(\psi_{i+1},\theta_{i+1})=0$, $i=1,\ldots,n$, subject to the periodic boundary condition $(\psi_{n+1},\theta_{n+1})=(\psi_1,\theta_1)$. This algorithm avoids exponential growth of error with UPO length, which occurs in solving the fixed point equation $F^n(\psi,\theta)-(\psi,\theta)=0$, and allows one to calculate arbitrarily long UPOs to any given accuracy. We find that a time series of 10^6 collisions is sufficient to determine all UPOs with seven and fewer collisions. The number of prime UPOs with 1–7 collisions and the corresponding n-collision approximants of the conductivity $\kappa_{(n)}$ are given in Table I. As shown in Fig. 2, the convergence of the approximants is slow and oscillatory. The convergence is greatly improved by means of the Shanks transformation [20] which eliminates the most pronounced transient of the form cq^n, $|q|<1$. All members of the transformed sequence are within 2% of our best estimate 0.100, which is obtained

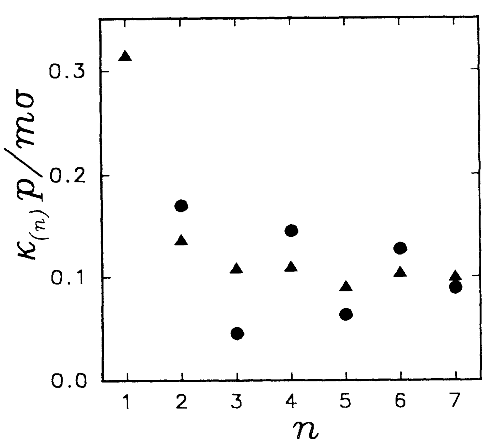

FIG. 2. The conductivity κ as a function of the order n of the approximant (the UPO collision length). The circles (triangles) are the results of full (symmetry-reduced) UPOs.

from symmetry-reduced cycles discussed below. This result also agrees with the estimate 0.101, which is obtained from a linear extrapolation of the data in Ref. [10].

In addition to time reversibility, the equations of motion possess another reflection symmetry $\mathcal{R}$: $(x,y,\theta)\to(x,-y,-\theta)$. The phase space can be reduced to half of a hexagonal cell by identifying points related through the symmetry $\mathcal{R}$. UPOs that are invariant under $\mathcal{R}$ in the full phase space are UPOs of half the length in the reduced phase space. For a given collision length, one expects symmetry-reduced UPOs to approximate the attractor better than nonreduced UPOs. This is born out by the faster convergence of $\kappa_{(n)}$ calculated with symmetry-reduced UPOs, which is plotted as triangles in Fig. 2.

The multifractal structure [21,22] of nonequilibrium flows [17] can also be understood in terms of the transport and stability properties of UPOs. We restrict our attention to the cross section of the attractor on the collision surface. The natural measure on this surface can be approximated by fixed points of higher and higher iterates of the collision mapping F (i.e., UPOs of longer and longer lengths). Consider the nth iterate F^n, and let j be an index labeling the fixed points of F^n (j determines a UPO). The pointwise dimension [15,21] (at a point X) is defined through

$$D_p(x)=\lim_{r\to 0}\log[\mu(B_X(r))]/\log r\,,$$

where $\mu(B_X(r))$ is the physical measure in a ball of radius r about X. The pointwise dimension for a point X on the unstable manifold of j is related to the Liapunov exponents of j [15]: $D_p(X)=1-\lambda_{1j}/\lambda_{2j}$. Using (2), we obtain the following relation between $D_p(X)$, the current, and stable Liapunov exponent of the UPO determined by j:

$$D_p(X)=2+\frac{\beta E}{\lambda_{2j}}\frac{\Delta x_j}{\tau_j}\,. \tag{7}$$

Thus the direction of mass transport on a UPO governs the sign of $D_p(X)-2$: $D_p<2$ for forward orbits, $D_p>2$ for reverse orbits, and $D_p=2$ for orbits in $\mathcal{P}_0$. Further, the pointwise dimension of UPOs and their time reverses are simply related: If a UPO has an associated pointwise dimension $1-\lambda_1/\lambda_2\equiv\alpha$, its time reverse has the associated pointwise dimension $1-\lambda_2/\lambda_1=\alpha/(\alpha-1)$. The Hausdorff dimension [21,22] $f(\alpha)$ of the set of points X such that $D_p(X)=\alpha$ can be calculated from UPOs [15]. In particular, $f(\alpha)$ is the transition value of D for which

$$\Gamma_\alpha(D)=\lim_{\Delta\alpha\to 0}\lim_{n\to\infty}\sum_{\substack{j\\ \alpha+\Delta\alpha\geq D_p(X)\geq\alpha}}\Lambda_{2j}^{D-1}$$

changes from infinity to zero as D is increased in value, where the sum is restricted to UPOs which satisfy $\alpha+\Delta\alpha\geq D_p(X)\geq\alpha$. Summing over the time reverses of the UPOs j with $D_p=\alpha$ and using $\Lambda_{1j}^{1/(1-\alpha)}=\Lambda_{2j}$, we obtain the relation

$$f\left(\frac{\alpha}{\alpha-1}\right)=\frac{f(\alpha)+\alpha-2}{\alpha-1}. \qquad (8)$$

Therefore, one only needs to calculate the spectrum for $\alpha<2$, the other half can be obtained through (8). Note from (7) that the spectrum $f(\alpha)$ can be split into three sets $\alpha<2$, $\alpha=2$, and $\alpha>2$ according to the type of UPO used in the calculation $\mathcal{P}_+$, $\mathcal{P}_0$, and $\mathcal{P}_-$, respectively. Of special importance are the Hausdorff dimension D_0, the maximum of f $[f(\alpha_0)=D_0]$, and the information dimension D_1 $[f(\alpha_1)=\alpha_1=D_1]$. Taking into account the reversibility of the equations of motion in applying the methods of Ref. [15], one can show $D_0=2$. Using this result along with (8) one obtains a relation between α_1 and α_0: $\alpha_0=D_1/(D_1-1)$. Also from (2) and the Kaplan-Yorke conjecture [21], one can derive $D_1=2+\beta E^2\kappa(E)/\lambda_2(E)$. Therefore as E is increased above zero, α_0 and α_1 move away from the value 2 a distance proportional to E^2 with $\alpha_0>2$ and $\alpha_1<2$.

In conclusion, we have shown that transport and multifractal properties of nonequilibrium steady-state flows can be understood in terms of the topology and stability of UPOs. The macroscopic flow is created by the favoring, due to stability, of forward over reverse UPOs. This asymmetry in weights of forward and reverse orbits also determines the multifractal structure of the attractor. The theory presented is directly applicable to viscous and heat conducting nonequilibrium flows [7,8]. Further studies are needed to clarify convergence rates.

The author would like to thank W. G. Hoover and J. Keizer for useful comments and a critical reading of the manuscript. This work was supported by NSF Grants No. CHE86-18647 and No. CHE89-18422 and an INCOR grant from the CNLS (Los Alamos).

[1] P. Gaspard and G. Nicholis, Phys. Rev. Lett. **65**, 1693 (1990).
[2] P. Gaspard and F. Baras, in *Microscopic Simulation of Complex Hydrodynamic Phenomena*, NATO ASI, edited by M. Maréschal and B. L. Holian (Plenum, London, 1991).
[3] R. Artuso, Phys. Lett. A **160**, 528 (1991).
[4] S. Nosé, J. Chem. Phys. **81**, 511 (1984); Mol. Phys. **52**, 255 (1984).
[5] D. J. Evans, W. G. Hoover, B. H. Failor, B. Moran, and A. J. C. Ladd, Phys. Rev. A **28**, 1016 (1983).
[6] B. L. Holian, W. G. Hoover, and H. A. Posch, Phys. Rev. Lett. **59**, 10 (1987).
[7] W. G. Hoover, Phys. Rev. A **37**, 252 (1988).
[8] G. P. Morriss, Phys. Lett. A **122**, 236 (1987); **134**, 307 (1989).
[9] H. A. Posch and W. G. Hoover, Phys. Rev. A **38**, 473 (1988).
[10] D. J. Evans, E. G. D. Cohen, and G. P. Morriss, Phys. Rev. A **42**, 5990 (1990).
[11] J. H. Hannay and A. M. Ozorio de Almeida, J. Phys. A **17**, 3429 (1984).
[12] W. Parry, Commun. Math. Phys. **106**, 267 (1986).
[13] G. Gunaratne and I. Procaccia, Phys. Rev. Lett. **59**, 1377 (1987).
[14] P. Cvitanović, Phys. Rev. Lett. **61**, 2729 (1988).
[15] C. Grebogi, E. Ott, and J. A. Yorke, Phys. Rev. A **37**, 1711 (1988).
[16] B. Moran, W. G. Hoover, and S. Bestiale, J. Stat. Phys. **48**, 709 (1987).
[17] W. G. Hoover and B. Moran, Phys. Rev. A **40**, 5319 (1989).
[18] V. I. Arnol'd and M. B. Sevryuk, in *Nonlinear Phenomena in Plasma Physics and Hydrodynamics*, edited by R. Z. Sagdeev (Mir Publishers, Moscow, 1986).
[19] D. Auerbach, P. Cvitanović, J.-P. Eckmann, G. Gunaratne, and I. Procaccia, Phys. Rev. Lett. **58**, 2387 (1987).
[20] C. M. Bender and S. A. Orszag, *Advanced Mathematical Methods for Scientists and Engineers* (McGraw-Hill, New York, 1978).
[21] J.-P. Eckmann and D. Ruelle, Rev. Mod. Phys. **57**, 617 (1985).
[22] T. C. Halsey, M. J. Jensen, L. P. Kadanoff, I. Procaccia, and B. I. Shraiman, Phys. Rev. A **33**, 1141 (1986).